

# Effect of decentration and tilt on the image quality of aspheric intraocular lens designs in a model eye

Timo Eppig, Katja Scholz, André Löffler, Arthur Meßner, PhD, Achim Langenbucher, PhD

**PURPOSE:** To determine the impact of decentration and tilt on the imaging quality of aspheric intraocular lens (IOL) designs in a schematic model eye.

**SETTING:** Institute of Medical Physics, University of Erlangen-Nuremberg, Erlangen, Germany.

**METHOD:** A model eye was used to calculate the impact of misalignment on the imaging quality of 6 IOL designs. The crystalline lens in the model eye was replaced with IOL designs with 22.0 diopters nominal refractive power, and the anterior chamber depth (ACD) was set to the estimated ACD value provided by the manufacturer. The retinal position was optimized for the best image quality. The IOLs were decentered up to  $\pm 1.0$  mm and tilted up to  $\pm 5$  degrees relative to the line of sight. At each position, the modulation transfer function was recorded with 3.0 mm and 4.5 mm pupil diameters. The results between the IOL designs and those of the phakic model eye were then compared.

**RESULTS:** Aberration-correcting IOLs were very sensitive to decentration and tilt. However, the impact of misalignment depended on IOL design. Aberration-free IOLs showed less sensitivity within a wide range of displacement but provided better results than the spherical IOL.

**CONCLUSIONS:** Overall, modern aspheric IOLs provided better imaging quality than conventional spherical IOL designs. Aberration-free IOLs were less sensitive to decentration and tilt than aberration-correcting IOLs but provided better image quality than spherical IOLs. Aberration-correcting IOLs have the potential to provide diffraction-limited imaging quality when perfectly aligned.

*J Cataract Refract Surg 2009; 35:1091–1100 © 2009 ASCRS and ESCRS*

For several years, aspheric intraocular lenses (IOLs) have been used in clinical practice to improve visual quality after cataract surgery.<sup>1–3</sup> Several approaches to designing aspheric IOLs have been described.<sup>4–8</sup> Today, 2 concepts of aspheric IOL designs are available.<sup>2,7,8</sup> One design corrects the intrinsic spherical aberration of the IOL in contrast to conventional spherical IOL designs; these IOLs are often referred to as aberration-free IOLs. The second design corrects cornea-induced spherical aberration; these IOLs are often called aberration-correcting IOLs. To design such IOLs, it is important to know the individual corneal spherical aberration. Most IOL designs, therefore, are optimized using model eyes that reflect average biometrical and optical data for a large group of individuals; for example, the Gullstrand schematic model eye and its derivatives or the physiologically more accurate Liou-Brennan model eye (LBME).<sup>6–14</sup> The resulting IOL designs generate an average level of spherical aberration to provide correction for a wide range of

patients rather than to provide individual spherical aberration correction. Because any wavefront correction depends on exact alignment of the involved optical elements, it is important to evaluate the effect of decentration and tilt on aspheric IOL performance.

In the past decade, several clinical studies have determined the decentration and tilt of IOLs after cataract surgery.<sup>15–25</sup> Table 1 shows a selection of decentration and tilt results in studies of IOL displacement. We extracted the mean absolute values for decentration and tilt based on the data in the table. In general, the mean decentration in the studies is  $0.30 \text{ mm} \pm 0.16$  (SD) (range 0.00 to 1.09 mm) and the mean tilt,  $2.62 \pm 1.14$  degrees (range 0.20 to 8.17 degrees). Most of the studies give only the absolute value of IOL decentration and tilt without the direction and sign. The studies in Table 1 were performed using 2 types of measuring systems: (1) Scheimpflug imaging (Nidek EAS-1000 and Oculus Pentacam) and (2) purpose-built Purkinje imaging devices. de Castro et al.<sup>24</sup> performed

cross-validation of those 2 modalities, which showed good comparability. In addition to the heterogeneous methods, the reference axes of the data differ, making comparisons difficult. Some studies used the pupillary axis as a reference for tilt and decentration, and others used the visual axis, which almost coincides with the line of sight for infinite object distances.<sup>14</sup>

Tabernero et al.,<sup>22</sup> Rosales and Marcos,<sup>23</sup> and de Castro et al.<sup>24</sup> provided information on the direction and sign of displacement. Tabernero et al.<sup>22</sup> found that temporal decentration and tilt occurred more often than nasal decentration and tilt in a study of 7 eyes. The data on the direction of horizontal decentration are supported by the data obtained by Rosales and Marcos.<sup>23</sup> However, they also found differences between right and left eyes and a significant amount of vertical decentration in a small sample (16 eyes). In contrast, de Castro et al.<sup>24</sup> report that nasal decentration and tilt seemed to occur more often (21 eyes).

In addition to the clinical studies of IOL misalignment, the literature describes several theoretical and in vitro experimental methods to determine the effect of misalignment of IOLs on imaging quality.<sup>26-30</sup> The purpose of this study was to evaluate the effect of decentration and tilt on the image quality of 5 commercially available aspheric IOLs and 1 spherical IOL (as a basic reference) using geometrical optics.

## MATERIALS AND METHODS

For the simulation of IOL performance, a model eye (LBME<sup>11</sup>) was used in which the gradient index lens was replaced by the respective IOL. The eye model is characterized by aspheric corneal elements; a gradient index crystalline lens; an iris pupil, which is decentered nasally by 0.50 mm;

and a visual axis, which is tilted by 5 degrees ( $\alpha$ ) relative to the optical axis.<sup>11</sup> The entrance pupil was calculated to be 3.10 mm from the anterior vertex of the cornea and its center displaced 0.59 mm nasally. The line of sight for simulating foveal imaging was implemented by rotating the complete model eye 5 degrees around the center of the entrance pupil. Because the crystalline lens in the original LBME is centered to the optical axis, the phakic eye model used in this study also incorporated slight crystalline lens decentration (approximately 0.50 mm temporally) and tilt (<5 degrees relative to the line of sight), which showed good agreement with recently published phakometric measurements by Rosales and Marcos<sup>23</sup> and Schaeffel.<sup>31</sup>

The LBME is supposed to be physiologically accurate and incorporates a realistic amount of spherical aberration, several effects (eg, Stiles-Crawford), and a realistic amount of chromatic aberration. However, the latter effects were not important in the simulations in this study because imaging quality was calculated for monochromatic green light (wavelength 555 nm) only and it has been shown that the Stiles-Crawford effect is negligible for image quality with small pupil diameters.<sup>32-34</sup> Liou and Brennan<sup>11</sup> did not provide a value for the retinal curvature because their model eye was designed for on-axis imaging only. However, the curvature of the retina may have an impact on image quality with displaced or tilted IOLs. A value of 12.0 mm was used for the retinal radius; this value was used by Atchison and Smith<sup>14</sup> for optical simulations with the LBME. Other model eyes use slightly different values for retinal curvature.

Calculations of imaging quality in terms of the modulation transfer function (MTF) were performed with the OSLO LT 6.1 optical design software (Lambda Research Corp.) for the visual axis of the model eye. The LBME was simulated (design data in Table 2) and then the gradient index lens element was replaced with the IOLs. Table 3 shows the design data and properties of the IOLs evaluated in this study. The IOL design data were provided by the manufacturers for the Aspira-aXA (MCX11ASP), MC6125AS, and MC5812AS. The data for the SofPort AO IOL were taken from an article by Altmann et al.<sup>30</sup> The data for the Tecnis Z9000 IOL were taken from the patent publication.<sup>7</sup> The surface data for the Invent ZO IOL was partially taken from the published patent application; although the center thickness of the lens was not provided, it could be derived using the manufacturer-supplied refractive index.<sup>8</sup> The Invent ZO IOL is of a material (hydrophilic acrylic) similar to that of the Aspira-aXA, MC6125AS, and MC5812AS IOLs; therefore, the same refractive index (1.461) was assumed and the center thickness was calculated for an edge thickness of 0.3 mm at the full optic diameter of 6.0 mm. This resulted in a center thickness of 1.107 mm. The optical performance results were in accordance with the simulation results supplied in the published patent application.<sup>8</sup>

The height  $z$  of the aspheric surfaces is defined as follows:

$$z = \frac{C \times \rho^2}{1 + \sqrt{1 - c^2(Q + 1) \times \rho^2}} + c_4 \rho^4 + c_6 \rho^6 + c_8 \rho^8 \quad (1)$$

where  $C$  is the surface curvature ( $C = 1/r$ ),  $\rho$  is the radial coordinate,  $Q$  is the conic constant ( $Q = -e^2$ ), and  $c_4$ ,  $c_6$ , and  $c_8$  are the higher-order aspheric coefficients.

The IOLs were placed in the posterior chamber. The estimated anterior chamber depth (ACD) (Table 3) was chosen for axial positioning of the IOLs. Because not all manufacturers supplied the ACD constant, the personalized ACD

Submitted: September 18, 2008.

Final revision submitted: January 16, 2009.

Accepted: January 26, 2009.

From the Medical Optics Research Group (Eppig, Scholz, Langenbucher), Institute of Medical Physics, University of Erlangen-Nuremberg, and the Max Planck Research School for Optics and Imaging (Eppig), Erlangen, and Dr. Schmidt Intraocularlinsen GmbH (Löffler, Meßner), Sankt Augustin, Germany.

Mr. Löffler and Dr. Meßner are employees of Dr. Schmidt Intraocularlinsen GmbH. No other author has a financial or proprietary interest in any material or method mentioned.

Supported by the International Max Planck Research School for Optics and Imaging, Erlangen, Germany.

Corresponding author: Timo Eppig, Medical Optics Research Group, Institute of Medical Physics at the University of Erlangen-Nuremberg, Henkestrasse 91, 91052 Erlangen, Germany. E-mail: timo.eppig@imp.uni-erlangen.de.

**Table 1.** Decentration and tilt data in recently published clinical studies of postoperative IOL dislocation. The studies by Rosales and Marcos<sup>23</sup> and de Castro et al.<sup>24</sup> provide additional information about the direction of tilt and decentration.

Source* (Year)	IOL	Eyes (n)	Mean FU (Mo) (Range)	Measurement Method	Reference Axis	Mean Absolute Decentration [mm]	Mean Absolute Horizontal Tilt [Degree]
Kim <sup>16</sup> (2001)	MZ60BD <sup>†</sup>	65	6	Scheimpflug	Pupillary	0.31 ± 0.15	2.67 ± 0.84
	SI-30NB <sup>‡</sup>	47		EAS-1000		0.32 ± 0.18	2.61 ± 0.83
	AcrySof MA60BM <sup>†</sup>	25				0.33 ± 0.19	2.69 ± 0.87
Taketani <sup>18</sup> (2004)	AcrySof MA30BA <sup>†</sup>	40	16.7 ± 14.4 (4–48)	Scheimpflug EAS-1000	Pupillary	0.30 ± 0.17	3.43 ± 1.55
	CeeOn 911A <sup>§</sup>	25	12	Scheimpflug	Visual	0.24 ± 0.13	3.03 ± 1.79
Baumeister <sup>21</sup> (2005)	PhacoFlex SI-40 <sup>§</sup>	25		EAS-1000		0.23 ± 0.13	3.26 ± 1.69
	CeeOn 911A <sup>§</sup>	28				0.29 ± 0.21	2.34 ± 1.81
	AcrySof MA60BM <sup>†</sup>	28				0.24 ± 0.10	2.32 ± 1.41
Mutlu <sup>19</sup> (2005)	AcrySof SA30AL <sup>†</sup>	45	27.1 ± 5.4 (19–34)	Purkinje	Pupillary	0.34 ± 0.08	2.70 ± 0.55
	AcrySof MA30BA <sup>†</sup>	43	26.7 ± 4.4 (20–34)	imaging		0.39 ± 0.13	2.72 ± 0.84
Rosales <sup>23</sup> (2006)	Unknown	16	—	Purkinje custom device	Pupillary	0.25 ± 0.28 (nasal)	0.87 ± 2.16 (nasal)
de Castro <sup>24</sup> (2007)	Unknown <sup>†,§,**</sup>	21	>6	Purkinje custom device	Pupillary	0.34 ± 0.19 (nasal)	2.34 ± 0.97 (nasal)
			>6	Scheimpflug Pentacam	Pupillary	0.23 ± 0.19 (nasal)	1.59 ± 0.82 (nasal)

Means ± SD  
 FU = follow-up; IOL = intraocular lens  
 \*First author  
<sup>†</sup>Alcon  
<sup>‡</sup>Allergan  
<sup>§</sup>Abbott Medical Optics, formerly Advanced Medical Optics  
<sup>\*\*</sup>Pharmacia

was derived from the A-constant, which was provided for all IOLs, using the following equation<sup>35</sup>:

$$pACD = A \times 0.62467 - 68.747 \quad (2)$$

where pACD is the personalized ACD constant and A is the A-constant used in the SRK formulas. The ACD values used for the simulations differed slightly from the pACD values, which can be explained by the inconsistency in the reference planes of the constants provided by the manufacturers. The center of the IOL was used as the reference plane, which is not coincident with the image-sided principal plane of the IOL; therefore, the pACD values in Table 3 may differ from the manufacturers' ACD values.

Focus optimization was performed using the auto-focus routine for minimum root mean square of the optical path difference for the perfectly aligned IOL (no decentration from the pupil center and no tilt relative to line of sight).

After optimization, the MTF feature of the OSLO optical design software was used to calculate the MTF through frequency in the tangential and sagittal directions. For finding a simple measure for the average image quality, the arithmetic mean between the tangential and sagittal MTFs was calculated. The optical design software provides MTF values in cycles/millimeter (cpmm) for focal imaging; thus, a transformation was applied to cycles/degree (cpd) as follows:

$$v_{[cpd]} = \left\{ \arctan \left[ (v_{[cpmm]} \times f_{air})^{-1} \right] \right\}^{-1} \quad (3)$$

where v is the spatial frequency and f<sub>air</sub> is the focal length of the eye in air.

To unify all calculations for the pseudophakic model eyes, a value of f<sub>air</sub> = 16.2 mm (16.5 mm for the phakic model eye) was used. For the desired optimization frequency of 30 cpd, the spatial frequency at the image plane yields approximately 106 cpmm (104 cpmm). Slight inaccuracies due to numerical rounding can be neglected. Displacement of the IOLs was performed as shown in Figure 1. To evaluate the influence of decentration, the IOLs were decentered in horizontal direction from -1.00 mm (temporal) to +1.00 mm (nasal) in steps of 0.25 mm relative to the pupil center. The respective MTF values were recorded for each decentration

**Table 2.** Optical design data of the phakic LBME used for simulation.

Surface	Radius (mm)	Conic Constant	Thickness (mm)	n (λ = 555 nm)
Anterior cornea	7.77	-0.18	0.50	1.376
Posterior cornea	6.40	-0.60	3.16	1.336
Iris	Infinity	—	0.00	1.336
Anterior lens	12.40	-0.94	1.59	1.368-1.407*
Posterior lens	Infinity	—	2.43	1.407-1.368*
Vitreous	-8.10	+0.96	16.27	1.336
Retina	-12.00	0.00	—	—

λ = wavelength; n = refractive index  
 \*Gradient index material modeled by the equations supplied by Liou and Brennan.<sup>11</sup> The retinal curvature was taken from Atchison and Smith.<sup>14</sup>

**Table 3.** Optical design data and properties of the tested IOLs.

Supplier	Advanced Medical Optics	Carl Zeiss Meditec AG	Human Optics AG	Dr. Schmidt Intraocularlinsen	Bausch & Lomb Inc.	Dr. Schmidt Intraocularlinsen
Product	Tecnis Z9000	Invent ZO	Aspira-aXA (MCX11ASP)	MC6125AS	SofPort AO	MC5812AS
Design concept	Aberration correcting	Aberration correcting	Aberration correcting	Aberration free	Aberration free	Spherical
Power (D)	22.0	22.0	22.0	22.0	22.0	22.0
Lens shape	Equiconvex	Biconvex	Biconvex	Biconvex	Biconvex	Biconvex
Anterior surface	6th-order asphere	Sphere	Sphere	Conic asphere	Conic asphere	Sphere
Radius (mm)	11.043	7.1497	10.83	12.0	7.285	13.0
Conic constant Q	-1.03613	0	0	-7.8	-1.085657	0
2nd-order coefficient $c_2$	0	0	0	0	0	0
4th-order coefficient $c_4$	-0.000944	0	0	0	0	0
6th-order coefficient $c_6$	-0.0000137	0	0	0	0	0
Posterior surface	Sphere	6th-order asphere	Conic asphere	Sphere	Conic asphere	Sphere
Radius (mm)	-11.043	-36.3903	-11.87	-10.733	-9.470	-10.0
Conic constant Q	0	0	-13.6	0	-1.085657	0
2nd-order coefficient $c_2$	0	-0.0068159	0	0	0	0
4th-order coefficient $c_4$	0	-0.0010213	0	0	0	0
6th-order coefficient $c_6$	0	-0.000062142	0	0	0	0
Center thickness (mm)	1.164	1.107*	1.0715	1.014	1.206	1.057
Refractive index	1.458	1.461*	1.461	1.461	1.427	1.461
Optic size (mm)	6.0	6.0	6.5	6.0	6.0	5.8
Optic material	Silicone	HPAC	HPAC	HPAC	Silicone	HPAC
Overall size (mm)	12.0	10.5	11.0	12.5	13.0	12.0
Haptic material	PVDF	HPAC	HPAC	HPAC	PMMA	HPAC
Haptic angulation (degrees)	6	0 – 10	0	0	5	0
Estimated ACD	5.4	5.09	5.15	5.2	4.96	5.2
Simulated pACD (mm)	5.11	5.4	5.15	5.29	5.37	5.35

ACD = anterior chamber depth; HPAC = hydrophilic acrylic; pACD = personalized anterior chamber depth used for simulation; PMMA = poly(methyl methacrylate); PVDF = polyvinylidene fluoride  
 \*Estimated values that showed excellent coincidence with the simulations supplied in the patent publication.<sup>8</sup>

value with 2 iris pupil diameters (3.0 mm and 4.5 mm) to address image quality for photopic vision and mesopic vision, respectively. In a second step, the IOLs were tilted relative to the line of sight from -5 degrees to +5 degrees in steps of 1 degree (Figure 1) to evaluate the effect of tilt on the MTF. Due to the huge amount of data, results for combined decentration and tilt are not presented here.

## RESULTS

### On-Axis Performance

The on-axis MTF was calculated for all IOLs to determine the difference between aberration-correcting, aberration-free, and spherical IOLs. Figure 2 shows the MTF plots with a 3.0 mm pupil. All 3 aberration-correcting IOLs (Tecnis Z9000, Zeiss ZO Design, Aspira-aXA) had a diffraction-limited MTF that was slightly better (104%) than that of the phakic LBME. The 2 aberration-free IOLs (MC6125AS, SofPort AO)

had slightly worse MTFs and yielded approximately 98% and 92% of the modulation of the phakic LBME at 30 cpd. The MTF of these 2 IOLs was limited by the spherical aberration of the cornea. The spherical IOL (MC5812AS) performed significantly worse than the other IOLs and yielded about only 76% of modulation of the phakic LBME at 30 cpd.

The differences between the IOL designs were more prominent with a 4.5 mm pupil. Figure 3 shows the respective MTF plots. The Tecnis Z9000 IOL, which yielded the highest amount of spherical aberration correction, had a better MTF than all other IOLs and than the phakic eye (183%). The Zeiss ZO and Aspira-aXA IOLs performed slightly better than the phakic eye (112% and 107%, respectively). The aberration-free IOLs (MC6125AS, SofPort AO) provided approximately 74% and 63%, respectively, of the modulation of the phakic eye at 30 cpd. Again, the

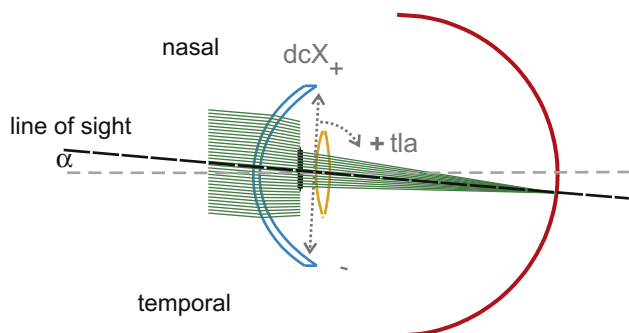


**Figure 1.** Schematic layout of the LBME with an implanted IOL. The coordinate system for decentration ( $dcX$ ) and tilt angle ( $tla$ ) is shown by the dashed lines. The line of sight was used as reference axis ( $\alpha$ ) for image quality and IOL tilt; IOL decentration was referred to the pupil center.

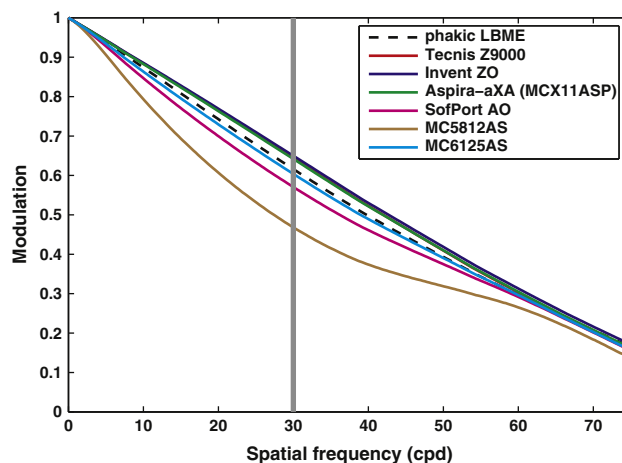
spherical IOL had the worst MTF (49%), which was the result of the spherical aberration of the IOL itself and of the cornea.

Table 4 shows detailed on-axis performance data.

### Decentration

Decentration led to poor MTF results in all cases except with the aberration-free IOLs (SofPort AO and MC6125AS) and the spherical IOL (MC5812AS). The degradation of modulation was significantly different for the IOL designs. Figure 4 shows the MTF results for decentration at 30 cpd with 3.0 mm and 4.5 mm pupils. With the 3.0 mm pupil size, all aberration-correcting IOLs had similar decentration behavior and the aberration-free IOLs were nearly insensitive to decentration; only the MC6125AS IOL showed a slight decay with larger decentration values. The performance of the spherical IOL (MC5812AS) was not affected by decentration.

With the 4.5 mm pupil, the amount of negative spherical aberration, the IOL design (position and order of aspheric surfaces), and the pupil size had a large impact on decentration sensitivity. The dominant error induced by decentration was horizontal coma followed by astigmatism and defocus. The Tecnis Z9000 IOL had the highest spherical aberration level and was therefore quite sensitive to decentration, even within the average decentration range. In contrast, the Aspira-aXA and the Invent ZO IOLs had lower spherical aberration levels and good MTF values within the average decentration range. Dependency of decentration on the MTF was not significant with the 2 aberration-free IOLs (MC6125AS and SofPort AO) within the average decentration range.



**Figure 2.** The MTF of all simulated IOLs and of the phakic LBME with a 3.0 mm pupil diameter. The vertical gray line indicates 30 cpd (visual acuity 20/20) (cpd = cycles per degree; LBME = Liou-Brennan model eye).

However, the imaging quality was slightly better with the MC6125AS than with the SofPort AO with the larger pupil. Again, decentration had no effect on the MTF with the spherical IOL.

The aberration-correcting IOLs yielded a significant increase in coma and astigmatism within the average displacement range of  $\pm 0.30$  mm, which increased with larger amounts of decentration.

### Tilt

Figure 5 shows the imaging quality of the IOLs as a function of lens tilt. Again, the Tecnis Z9000 IOL had the highest maximum modulation but also the greatest sensitivity to tilt. The differences were slight with the Aspira-aXA and Invent ZO IOLs, both designs provided better or equal MTF than the aberration-free IOLs and the spherical IOL within the average tilt angle of  $\pm 3$  degrees. The aberration-free IOLs and the spherical IOL were almost insensitive to tilt within that range. With all IOLs, the effect of tilt on the MTF was not as distinct as the effect of decentration.

### DISCUSSION

Ray tracing is a common and useful method of designing and theoretically testing optical components. We used an optical design software package to trace a bundle of rays through the widely accepted LBME,<sup>11</sup> which contains aspheric and gradient index elements as well as a decentered pupil, as is found in many human eyes. For simulating the optical performance of IOLs, we replaced the gradient index crystalline lens with commercially available artificial lenses. The design data of the IOLs were provided by IOL manufacturers

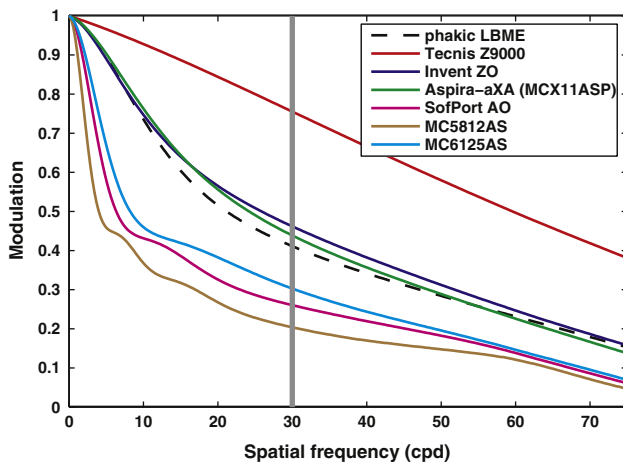


**Figure 3.** The MTF of all simulated IOLs and of the phakic LBME with a 4.5 mm pupil diameter. The vertical gray line indicates 30 cpd (visual acuity 20/20) (cpd = cycles per degree; LBME = Liou-Brennan model eye).

or taken from patent publications.<sup>7,8</sup> Calculations were performed with monochromatic green light (wavelength 555 nm), and the Stiles-Crawford effect was not considered because of its minimal influence on visual quality.<sup>32–34</sup>

We then decentered the implanted lens from  $-1.00$  mm (temporal) to  $+1.00$  mm (nasal) and calculated the tangential, sagittal, and average MTF at each position. The impact of vertical decentration was not evaluated; however, it would have a similar effect on image quality. Decentration results showed high image quality degradation in aberration-correcting IOLs. However, the amount of MTF degradation was also highly dependent on the individual IOL design. Of the aberration-correcting IOLs, the Aspira-aXA and Invent ZO had better MTF values on-axis and within  $\pm 0.3$  mm of decentration; however, when decentered more than  $\pm 0.5$  mm, their performance degraded to that of the spherical IOL. The Tecnis Z9000 IOL showed rapid degradation within the  $\pm 0.3$  mm range and worse results than the spherical IOL when decentered more than  $0.4$  mm. Our results agree with those of Altmann et al.<sup>30</sup> and Holladay et al.<sup>6</sup> The MTF values of the 2 aberration-free IOLs (MC6125AS and SofPort AO) showed less decentration dependency, and the MTF of the spherical IOL was independent of decentration.

In a second test, we tilted the IOLs from  $-5$  degrees (temporally) to  $+5$  degrees (nasally) around their anterior vertex and recorded the tangential, sagittal, and mean MTFs again. We found that the aberration-free IOLs and the spherical IOL provided almost constant imaging quality over a wide range of tilt. However, the MTF of the spherical IOL was significantly lower than that of the aberration-free IOLs. Aberration-correcting IOLs showed higher sensitivity to tilt. We

**Table 4.** Comparison of the on-axis MTF performance of the tested IOL designs relative to the MTF of the phakic LBME.

IOL Design	Relative MTF Performance at 30 cpd	
	3.0 mm Pupil	4.5 mm Pupil
Tecnis Z9000	1.044	1.834
Invent ZO	1.054	1.122
Aspira-aXA	1.041	1.065
MC6125AS	0.979	0.736
SofPort AO	0.925	0.632
MC5812AS	0.759	0.495
Reference: LBME	0.617	0.412

cpd = cycles per degree; LBME = Liou-Brennan model eye; MTF = modulation transfer function  
Reference: LBME are absolute values.

found that although aberration-correcting IOLs provided very good image quality, they may be sensitive to displacement and tilt. In contrast, aberration-free IOLs provided good image quality that was better than that of spherical IOLs and were as insensitive to displacement as common spherical IOLs. Our results agree with those of Altmann et al.<sup>30</sup> in a theoretical study of the Tecnis Z9000 and SofPort AO IOLs and a spherical IOL. In a clinical study of the visual outcomes in eyes with the Tecnis Z9000 IOL, Mester et al.<sup>36</sup> found an improvement in contrast sensitivity. Bellucci et al.<sup>37</sup> report a significant increase in visual acuity and contrast sensitivity in eyes that had a Tecnis Z9000 IOL compared with a conventional spherical IOL (AcrySof SA60AT, Alcon) at higher spatial frequencies (18 cpd). These results are also supported in a study by Packer et al.<sup>38</sup> However, no significant improvement in visual acuity with low and high contrast and a decrease in spherical aberration were found in 2 studies by Kasper et al.<sup>39,40</sup> Assuming that the IOLs in those studies were well centered, the results agree with the finding in our simulation that the Tecnis Z9000 IOL provided much better image quality than a spherical IOL. A recently published multicenter study in Sweden<sup>41</sup> compared the subjective outcomes in patients who had cataract surgery with implantation of an aberration-free Akreos Adapt AO IOL (Bausch & Lomb) in 1 eye and a Tecnis Z9000 IOL in the other eye. They found that 28% of the patients reported better subjective visual quality in the eye with the aberration-free IOL than in the eye with the aberration-correcting IOL (14%); 33% of the patients noticed more visual disturbances in the eye with the aberration-correcting IOL than in the eye with the aberration-free IOL (11%). These findings agree with our results, indicating that the aberration-free IOL has higher

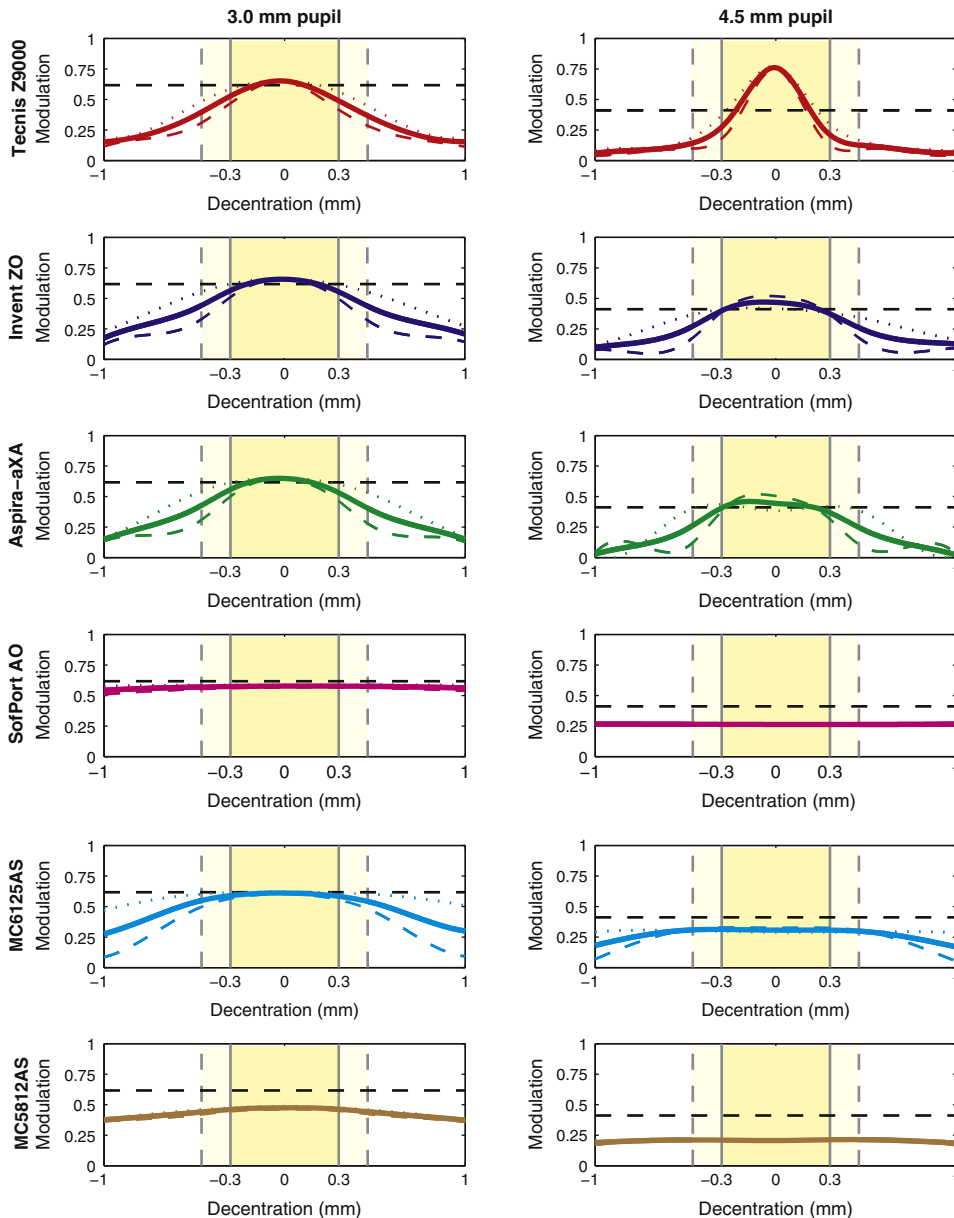


**Figure 4.** The MTF of the tested IOLs as a function of decentration with a 3.0 mm pupil (left column) and a 4.5 mm pupil (right column). The mean MTF (colored solid lines) is shown with the sagittal MTF (colored dotted lines) and tangential MTF (colored dashed lines). The mean decentration range in the literature (darker yellow bars with vertical solid lines) and the standard deviation (lighter yellow bars with vertical dashed lines) are shown. The MTF of the LBME without decentration (dashed black line) is plotted as reference.

performance stability than the aberration-correcting IOL and that the latter may provide inferior optical quality in some cases. To our knowledge, there are no recent clinical studies of the other IOLs that we evaluated; however, several studies of the outcomes of cataract surgery with aspheric IOLs have been published.<sup>36-41</sup> Furthermore, our results are supported by other studies<sup>27,42</sup> and by a recent experimental in vitro study of aspheric IOLs.<sup>43</sup>

The specific design of the aberration-correcting IOLs had a significant effect on their sensitivity to displacement. The Invent ZO IOL design was intended to be less sensitive to decentration than the design of other aberration-correcting IOLs. However, our simulations with the conceptual Invent ZO do not support this

statement, although the IOL seems to provide good image quality within a decentration range of  $\pm 0.5$  mm. The Aspira-aXA IOL yielded similar results and provided good image quality within the average decentration range. Both IOLs showed only slight sensitivity to tilt. The aberration-free IOLs and the spherical IOL had stable image quality within the complete range of decentration ( $\pm 1.00$  mm). The influence of tilt was small with those IOLs. In addition to aberration-correcting IOLs, other IOL designs showed differences between models. For example, there was a considerable difference between the aberration-free IOLs designs; the IOL with the anterior and posterior aspherics was more robust to decentration than the IOL with the single anterior aspheric. In general, the aberration

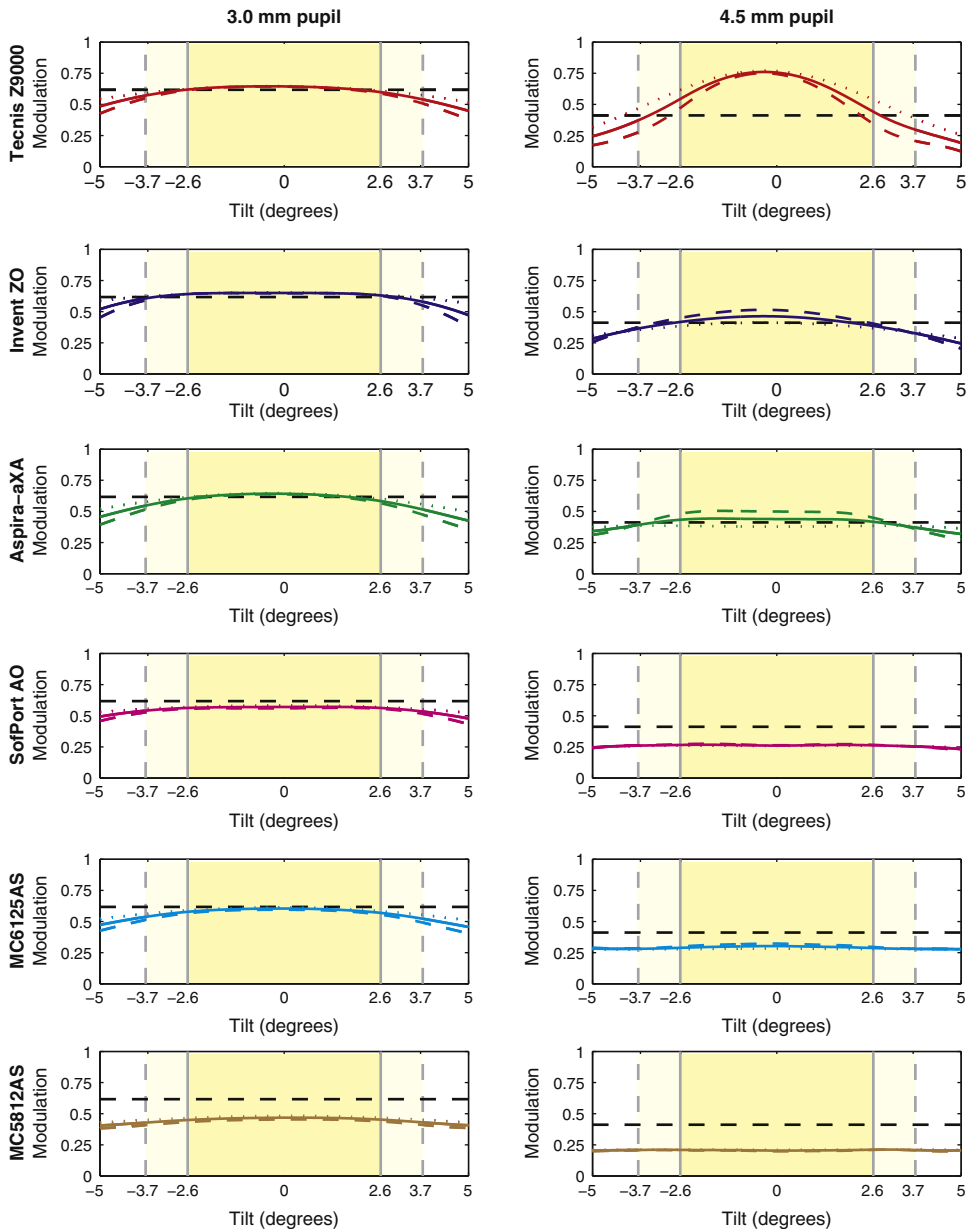


**Figure 5.** The MTF of the tested IOLs as a function of tilt with a 3.0 mm pupil (left column) and a 4.5 mm pupil (right column). The mean MTF (colored solid lines) is shown with the sagittal MTF (colored dotted lines) and tangential MTF (colored dashed lines). The mean tilt range in the literature (darker yellow bars with vertical solid lines) and the standard deviation (lighter yellow bars with vertical dashed lines) are shown. The MTF of the LBME without tilt (dashed black line) is plotted as reference.

correction should be set to the posterior surface or both surfaces.

Our study was restricted to a theoretical model eye; therefore, our results cannot be used for realistic prediction of surgical outcomes. Individual computer model eyes based on real biometric data are needed for concise study of misalignment of aspheric IOLs and better prediction of individual visual outcomes of cataract surgery, as proposed in previous studies.<sup>13,22,44</sup> Our methods were similar to those of Altmann et al.<sup>30</sup>; however, we used a different model eye and presented the MTF at 30 cpd against the amount of misalignment instead of showing complete MTF curves for discrete values of misalignment. Our study provides an overview of current IOL design

concepts and their theoretical performance stability under misalignment conditions. Therefore, our work can be considered an extension of previous studies.<sup>28-30</sup>

In addition, we did not evaluate the effect of combined decentration and tilt, which is present in most pseudophakic eyes. However, we performed a simulation with combined decentration and tilt; the simulation showed that both displacement factors partially compensate for their negative effects on the MTF. This compensatory effect was also reported by Barbero et al.<sup>26</sup> and explains why such aberration-correcting IOLs often work well without inducing visual disturbances. In a more recent article, Marcos et al.<sup>45</sup> discussed a passive mechanism for compensation of horizontal

coma in pseudophakic eyes. This concept is interesting because it implies compensation for errors induced by slight horizontal decentration of aspheric IOLs.

In clinical practice, the causes of postoperative IOL dislocation are not fully understood. The several clinical studies of the possible causes of IOL dislocation propose many influencing variables.<sup>46-50</sup> Pathological factors such as posterior capsule opacification, capsular bag instability, and anterior capsule fibrosis may cause IOL decentration and tilt. However, surgical technique and IOL haptic design seem to have the most influence on IOL stability.<sup>46,47</sup> In cataract surgery, the extent of postoperative IOL dislocation may be minimized by using a technique that includes continuous curvilinear capsulorhexis rather than the intracapsular cataract extraction method (envelope technique). Capsular bag shrinkage after postoperative IOL dislocation may be prevented by the use of capsular tension rings.<sup>51,52</sup>

In conclusion, aspheric IOLs provided better imaging quality than spherical IOLs; however, imaging quality may be very sensitive to decentration or tilt depending on the aberration correction concept of the IOL design. If the mean decentration can be limited to  $\pm 0.3$  mm, the aberration-correcting IOL concept provides, more or less, diffraction-limited imaging quality at 30 cpd, which equals a visual acuity of 20/20. If exact alignment cannot be guaranteed in cases with persisting pathologies, aberration-free IOLs may be a good choice to provide the patient with an acceptable compromise between good imaging quality and a design that is robust to decentration and tilt. We suggest that surgeons use a more robust IOL design when proper alignment of the IOL cannot be guaranteed.

## REFERENCES

- Bellucci R, Morselli S. Optimizing higher-order aberrations with intraocular lens technology. *Curr Opin Ophthalmol* 2007; 18:67-73
- Kohnen T, Klaproth OK. Asphärische Intraokularlinsen. [Aspheric intraocular lenses]. *Ophthalmologe* 2008; 105:234-240
- Werner L, Olson RJ, Mamalis N. New technology IOL optics. *Ophthalmol Clin North Am* 2006; 19(4):469-483
- Lu CW, Smith G. The aspherizing of intra-ocular lenses. *Ophthalmic Physiol Opt* 1990; 10:54-66
- Atchison DA. Design of aspheric intraocular lenses. *Ophthalmic Physiol Opt* 1991; 11:137-146
- Holladay JT, Piers PA, Koranyi G, van der Mooren M, Norrby NES. A new intraocular lens design to reduce spherical aberration of pseudophakic eyes. *J Refract Surg* 2002; 18:683-691
- Norrby N, Artal P, Piers PA, van der Mooren M. inventors; Pharmacia Groningen BV, assignee. Methods of obtaining ophthalmic lenses providing the eye with reduced aberrations. US patent 863546, 2001. Available at: <http://www.patentstorm.us/patents/6609793/fulltext.html>. Accessed February 10, 2009
- Gerlach M, Lesage C, inventors. Carl Zeiss Meditec AG, assignee. Asphärische künstliche Augenlinse und Verfahren für die Konstruktion einer solchen. German patent application DE10 2006 021521 A1 November 8, 2007. Available at: <http://www.patent-de.com/20071108/DE102006021521A1.html>. Accessed February 10, 2009
- Gullstrand A. Appendix part 1. In: Helmholtz H. *Handbuch der Physiologischen Optik*, 3d ed. Hamburg, Leipzig, Germany, Leopold Voss; 350-358
- Lotmar W. Theoretical eye model with aspherics. *J Opt Soc Am* 1971; 61:1522-1529
- Liou H-L, Brennan NA. Anatomically accurate, finite model eye for optical modeling. *J Opt Soc Am A* 1997; 14:1684-1695
- Tabernero J, Piers P, Artal P. Intraocular lens to correct corneal coma. *Opt Lett* 2007; 32:406-408
- Rosales P, Marcos S. Customized computer models of eyes with intraocular lenses. *Opt Express* 2007; 15:2204-2218. Available at: <http://www.opticsinfobase.org/abstract.cfm?URI=oe-15-5-2204>. Accessed February 10, 2009
- Atchison DA, Smith G. *Optics of the Human Eye*. Oxford, UK, Boston, MA, Butterworth-Heinemann, 2002
- Jung CK, Chung SK, Baek NH. Decentration and tilt: silicone multifocal versus acrylic soft intraocular lenses. *J Cataract Refract Surg* 2000; 26:582-585
- Kim JS, Shyn KH. Biometry of 3 types of intraocular lenses using Scheimpflug photography. *J Cataract Refract Surg* 2001; 27:533-536
- Nejima R, Miyata K, Honbou M, Tokunaga T, Tanabe T, Sato M, Oshika T. A prospective, randomised comparison of single and three piece acrylic foldable intraocular lenses. *Br J Ophthalmol* 2004; 88:746-749
- Taketani F, Matsuura T, Yukawa E, Hara Y. Influence of intraocular lens tilt and decentration on wavefront aberrations. *J Cataract Refract Surg* 2004; 30:2158-2162
- Mutlu FM, Erdurman C, Sobaci G, Bayraktar MZ. Comparison of tilt and decentration of 1-piece and 3-piece hydrophobic acrylic intraocular lenses. *J Cataract Refract Surg* 2005; 31:343-347
- Taketani F, Yukawa E, Yoshii T, Sugie Y, Hara Y. Influence of intraocular lens optical design on high-order aberrations. *J Cataract Refract Surg* 2005; 31:969-972
- Baumeister M, Neidhardt B, Strobel J, Kohnen T. Tilt and decentration of three-piece foldable high-refractive silicone and hydrophobic acrylic intraocular lenses with 6-mm optics in an intraindividual comparison. *Am J Ophthalmol* 2005; 140:1051-1058
- Tabernero J, Piers P, Benito A, Redondo M, Artal P. Predicting the optical performance of eyes implanted with IOLs to correct spherical aberration. *Invest Ophthalmol Vis Sci* 2006; 47:4651-4658. Available at: <http://www.iovs.org/cgi/reprint/47/10/4651>. Accessed February 10, 2009
- Rosales P, Marcos S. Phakometry and lens tilt and decentration using a custom-developed Purkinje imaging apparatus: validation and measurements. *J Opt Soc Am A* 2006; 23:509-520
- de Castro A, Rosales P, Marcos S. Tilt and decentration of intraocular lenses in vivo from Purkinje and Scheimpflug imaging; validation study. *J Cataract Refract Surg* 2007; 33:418-429
- Oshika T, Sugita G, Miyata K, Tokunaga T, Samejima T, Okamoto C, Ishii Y. Influence of tilt and decentration of scleral-sutured intraocular lens on ocular higher-order wavefront aberration. *Br J Ophthalmol* 2007; 91:185-188
- Barbero S, Marcos S, Jiménez-Alfaro I. Optical aberrations of intraocular lenses measured in vivo and in vitro. *J Opt Soc Am A* 2003; 20:1841-1851
- Dietze HH, Cox MJ. Limitations of correcting spherical aberration with aspheric intraocular lenses. *J Refract Surg* 2005; 21:S541-S546
- Kozaki J, Takahashi F. Theoretical analysis of image defocus with intraocular lens decentration. *J Cataract Refract Surg* 1995; 21:552-555

29. Turuwhenua J. A theoretical study of intraocular lens tilt and decentration on perceptual image quality. *Ophthalmic Physiol Opt* 2005; 25:556–567
30. Altmann GE, Nichamin LD, Lane SS, Pepose JS. Optical performance of 3 intraocular lens designs in the presence of decentration. *J Cataract Refract Surg* 2005; 31:574–585
31. Schaeffel F. Binocular lens tilt and decentration measurements in healthy subjects with phakic eyes. *Invest Ophthalmol Vis Sci* 2008; 49:2216–2222
32. Stiles WS, Crawford BH. The luminous efficiency of rays entering the eye pupil at different points. *Proc R Soc Lond [Biol]*; 1933; 112:428–450
33. van Meeteren A. Calculations on the optical modulation transfer function of the human eye for white light. *Optica Acta* 1974; 21:395–412
34. Atchison DA, Scott DH, Joblin A, Smith G. Influence of Stiles-Crawford effect apodization on spatial visual performance with decentered pupils. *J Opt Soc Am A* 2001; 18:1201–1211
35. Retzlaff JA, Sanders DR, Kraff MC. Development of the SRK/T intraocular lens implant power calculation formula. *J Cataract Refract Surg* 1990; 16:333–340; correction, 528
36. Mester U, Dillinger P, Anterist N. Impact of a modified optic design on visual function: clinical comparative study. *J Cataract Refract Surg* 2003; 29:652–660
37. Bellucci R, Scialdone A, Buratto L, Morselli S, Chierigo C, Criscuoli A, Moretti G, Piers P. Visual acuity and contrast sensitivity comparison between Tecnis and AcrySof SA60AT intraocular lenses: a multicenter randomized study. *J Cataract Refract Surg* 2005; 31:712–717; errata, 1857
38. Packer M, Fine IH, Hoffman RS, Piers PA. Improved functional vision with a modified prolate intraocular lens. *J Cataract Refract Surg* 2004; 30:986–992
39. Kasper T, Bühren J, Kohnen T. Aberrationen höherer Ordnung nach Implantation von asphärischen und sphärischen Intraokularlinsen in Abhängigkeit von der Pupillenweite. [Intraindividual comparison of higher order aberrations after implantation of aspherical and spherical IOLs depending on pupil diameter]. *Ophthalmologe* 2005; 102:51–57
40. Kasper T, Bühren J, Kohnen T. Intraindividual comparison of higher-order aberrations after implantation of aspherical and spherical intraocular lenses as a function of pupil diameter. *J Cataract Refract Surg* 2006; 32:78–84
41. Johansson B, Sundelin S, Wikberg-Matsson A, Unsbo P, Behndig A. Visual and optical performance of the Akreos Adapt Advanced Optics and Tecnis Z9000 intraocular lenses; Swedish multicenter study. *J Cataract Refract Surg* 2007; 33:1565–1572
42. Wang L, Koch DD. Effect of decentration of wavefront-corrected intraocular lenses on the higher-order aberrations of the eye. *Arch Ophthalmol* 2005; 123:1226–1230
43. Pieh S, Fiala W, Malz A, Stork W. In vitro Strehl ratios with spherical, aberration free, average and customized spherical aberration correcting intraocular lenses. *Invest Ophthalmol Vis Sci* 2009; 50:1264–1270
44. Piers PA, Norrby NES, Mester U. Eye models for the prediction of contrast vision in patients with new intraocular lens designs. *Opt Lett* 2004; 29:733–735
45. Marcos S, Rosales P, Llorente L, Barbero S, Jiménez-Alfaro I. Balance of corneal horizontal coma by internal optics in eyes with intraocular artificial lenses: evidence of a passive mechanism. *Vision Res* 2008; 48:70–79
46. Akkin C, Özler SA, Menten J. Tilt and decentration of bag-fixated intraocular lenses: a comparative study between capsulorhexis and envelope techniques. *Doc Ophthalmol* 1994; 87:199–209
47. Caballero A, Losada M, Lopez JM, Gallego L, Sulla O, Lopez C. Decentration of intraocular lenses implanted after intercapsular cataract extraction (envelope technique). *J Cataract Refract Surg* 1991; 17:330–334
48. Hayashi K, Hayashi H, Nakao F, Hayashi F. Comparison of decentration and tilt between one piece and three piece polymethyl methacrylate intraocular lenses. *Br J Ophthalmol* 1998; 82:419–422
49. Mutlu FM, Bilge AH, Altinsoy HI, Yumusak E. The role of capsulotomy and intraocular lens type on tilt and decentration of polymethylmethacrylate and foldable acrylic lenses. *Ophthalmologica* 1998; 212:359–363
50. Tappin MJ, Larkin DF. Factors leading to lens implant decentration and exchange. *Eye* 2000; 14:773–776
51. Takimoto M, Hayashi K, Hayashi H. Effect of a capsular tension ring on prevention of intraocular lens decentration and tilt and on anterior capsule contraction after cataract surgery. *Jpn J Ophthalmol* 2008; 52:363–367
52. Lee D-H, Shin S-C, Joo C-K. Effect of a capsular tension ring on intraocular lens decentration and tilting after cataract surgery. *J Cataract Refract Surg* 2002; 28:843–846



First author:  
Timo Eppig

*Medical Optics Research Group, Institute of Medical Physics, University of Erlangen-Nuremberg, and Max Planck Research School for Optics and Imaging, Erlangen, Germany*